JOM, Vol. 65, No. 7, 2013
DOI: 10.1007/s11837-013-0620-5

Microstructure Control of $L1_0$-Ordered FePt Granular Film for Heat-Assisted Magnetic Recording (HAMR) Media

B.S.D.Ch.S. VARAPRASAD,[1,2] Y.K. TAKAHASHI,[1] and K. HONO[1]

1.—National Institute for Materials Science, 1-2-1, Sengen, Tsukuba 305-0047, Japan.
2.—e-mail: b.varaprasad@nims.go.jp

$L1_0$-ordered FePt nanogranular film is one of the promising candidates for the next-generation high areal density media for heat-assisted magnetic recording (HAMR). To realize a suitable microstructure for the HAMR media, the granular structure composed of uniformly dispersed $L1_0$-FePt nanoparticles with various segregants has been optimized using various combinations of segregants and seed layer materials. Although the microstructure of FePt-C came so close to the ideal one for HAMR, it would not be the final answer as the growth of the columnar grain structure is not possible due to too strong phase separation between FePt and C. In this article, we review recent investigations aiming at achieving the ideal microstructure for HAMR media.

INTRODUCTION

A hard-disk drive (HDD) is a data storage device that stores digital information by magnetizing nanosized ferromagnets on flat disks and retrieves data by sensing the magnetic field from them. HDDs have been a major storage device in computers for the past 50 years due to their large capacity, low cost, and nonvolatility. Although solid-state devices (SSDs) are now replacing storage devices for portable computers, HDDs will continue to be a major player in the data storage industry as only HDDs can meet the demand to store rapidly increasing digital data for cloud computing. The number of HDDs sold in 2012 was approximately 800 million, nearly one tenth of the world population!

An HDD is composed of one or more rigid disks with magnetic heads supported on actuator arms to write and read digital information. The disk rotates at a very fast rate (~7000 rpm), and a small magnetoresistive head flies on the disk with a distance of a few nanometers. The areal density of recording is the number of bits per square inch (bit/in^2) and that of the current HDD is approximately 700 Gbit/in^2. The higher the areal density, the more data we can store in the same volume, leading to reductions in size and energy consumption. In the past, the areal density of HDD had shown an increase of 100% every year, but the recent growth rate has slowed to 30% reaching saturation.[1] Although various technological improvements have been made in both recording heads and media in the current perpendicular recording (PMR) system, ~1 Tbit/in^2 is considered to be the limit for the PMR method. Thus, a transition to a new magnetic recording method must be achieved in the near future to sustain the recording industry.

Heat-assisted magnetic recording (HAMR) is a technology closer to commercialization. However, a new medium that is totally different from the current one must be developed using a high-magnetocrystalline anisotropy material. The current recording media are CoCrPt-SiO_2 nanogranular films, in which nanosized CoCrPt columnar grains with the hexagonal close-packed structure are dispersed uniformly with a strong [0001] fiber texture as shown in Fig. 1. Such films are deposited on glass substrates with an amorphous CoTaZr soft magnetic underlayer* (SUL) and the Ru seed layer that optimizes the grain size and the crystallographic orientation of the CoCrPt grains. Because the easy axis of magnetization of the CoCrPt alloy is the [0001] direction, this crystallographic texture gives rise to a strong perpendicular magnetic anisotropy. Each grain is magnetically isolated, and one bit contains multiple CoCrPt grains that are magnetized in the same direction as shown in Fig. 2. The

*To maximize the magnetic field generated from a write pole, a soft magnetic layer is placed under the hard magnetic granular recording layer so that the magnetix flux make a closure loop from the read pole to a return pole in PMR media.

(Published online May 31, 2013)

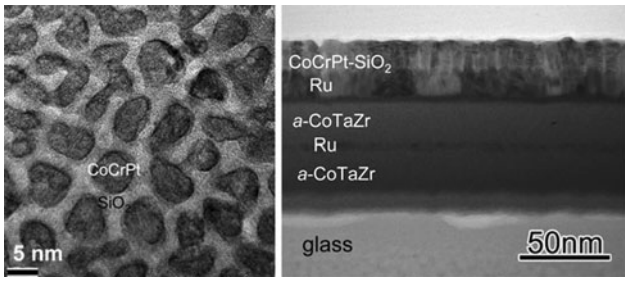

Fig. 1. Transmission electron microscopy planar image of the CoCrPt-SiO_2 recording layer and the cross-sectional image of the currently used perpendicular recording media. CoCrPt ferromagnetic particles of ~6 nm are dispersed in SiO_2. On the glass substrate, amorphous-CoTaZr softmagnetic underlayer and the Ru interlayer that align the [0001] axis in the perpendicular to the film are grown. The CoCrPt grains are grown on Ru grains epitaxially with the strong [0001] texture.

bit size of the areal density of 1 Tbit/in^2 will be $\sim 25 \times 25$ nm^2, in which more than 10 ferromagnetic particles must be contained to obtain a sufficient signal-to-noise ratio. This means that the ferromagnetic particles must be refined further to ~4 nm for an areal density above 1 Tbit/^{2}. This requirement makes the ferromagnetic particles thermally unstable as the magnetocrystalline energy K_uV becomes comparable to the thermal energy k_BT, where K_u is the uniaxial magnetocrystalline energy, V is the volume of the particle, and k_B is the Boltzmann constant. To keep the recorded information for longer than 10 years, K_uV/k_BT must be larger than 60. This means that the ferromagnetic material with high magnetocrystalline anisotropy such as $L1_0$-FePt, $L1_0$-CoPt, $Nd_2Fe_{14}B$, and $SmCo_5$ must be used for high density recording where V becomes as small as $\sim 6 \times 10^{-28}$ m^3.[2,3] As the media require long-term endurance, the rare-earth compounds are unlikely to be selected as they are very susceptible to corrosion. As a result, $L1_0$-FePt phase is currently considered to be most promising material for HAMR media.

Although the K_u of CoCrPt alloys is ~0.3 MJ/m^3, the $L1_0$-ordered FePt has an order of magnitude larger magnetocrystalline anisotropy of 6.6 MJ/m^3, which makes the minimum size of stable ferromagnetic particles ~4 nm for spheres and 2.4 nm for cylinders.[4] However, if we make the hard magnetic particles so small, then the magnetic field required to switch the magnetization of the particle or coercivity (μ_0H_c) will increase enormously. The typical switching field or μ_0H_c for the current recording media is about 0.8 T, whereas μ_0H_c of the nanosized hard magnet will be higher than 3 T. The highest magnetic field that can be generated using a write head (a small electromagnet with a soft magnetic "write pole") is limited to about 1.5 T using the soft ferromagnet with the highest saturation magnetic flux density of 2.35 T for $Fe_{65}Co_{35}$.[5] This means that the nanosized particles of hard magnetic materials are not writable. This is known as "trilemma" of magnetic recording; ultrahigh-density magnetic recording requires nanosized ferromagnetic particles, and then they become thermally unstable. To overcome this problem, a high K_u material must be used; however, the switching field of the particles becomes too large to write.

To break out of the trilemma, the magnetization switching must be assisted by some external energy. The HAMR uses heat to assist the magnetization switching of high K_u particles with thermal energy using a well-focused laser beam as shown in Fig. 3a.[6,7] As temperature increases, the coercivity of the particles decreases because of reduced magnetocrystalline anisotropy as shown in Fig. 3b. Writing is done at the temperature slightly lower than Curie temperature where the coercive field becomes small than the write field. When temperature decreases after writing, the high K_u nanosized particle has sufficient thermal stability for permanent recording.

HAMR MEDIA

To realize HAMR, new technologies in both the head and the medium are necessary. The HAMR head has been demonstrated recently using a plasmonic antenna.[6] However, a suitable magnetic recording medium to demonstrate the feasibility of high-density HAMR recording had not been successfully produced until recently. The desirable HAMR media should be composed of densely dispersed ferromagnetic particles of high-magnetocrystalline anisotropy with a uniform particle size of 4 nm to 6 nm with columnar grains of the aspect ratio $D/h > 1.5$ as shown in Fig. 2. The film must exhibit high coercivity above 3 T, more than four times larger than that of the current recording media, with a small size distribution or a switching field distribution** (SFD). In addition, the microstructure should be realized on commercially viable substrates such as glass at low processing temperatures. The key factors to control for HAMR media are (I) ordering of the FePt phase to the $L1_0$ structure, (II) obtaining magnetic perpendicular anisotropy, (III) attaining nanometer diameter with a narrow size distribution as described below.

$L1_0$ Order of FePt

$L1_0$ ordering in FePt films is crucial to achieve the high-magnetocrystalline anisotropy. Although the $L1_0$-FePt structure reaches thermally equilibrium below 1300°C, FePt films sputter-deposited below 550°C are disordered to the A1 phase because of the kinetic constraint. Because the melting temperature of equiatomic FePt alloy is about 1830 K, the volume diffusion is very sluggish below 917 K (~640°C). This means that the sputtered A1 film

**Because coercivity varies depending on the size and the degree of $L1_0$ order of ferromagnetic particles, the size dispersion causes large SFD. This is not desirable for reliable recording.

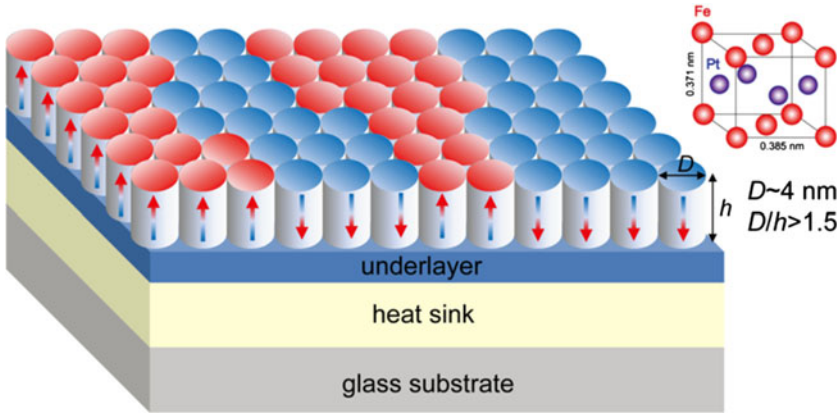

Fig. 2. Ideal media structure for HAMR. Red and blue colors show the direction of magnetic poles and their boundary is the magnetic domains that separate the neighboring bits. The $L1_0$-FePt (the upper right figure) must grow columnarly separated by the nonferromagnetic "segregant." The column diameter and height ratio *D*/*h* must be higher than 1.5 and a diameter of less than 4 nm is desired.

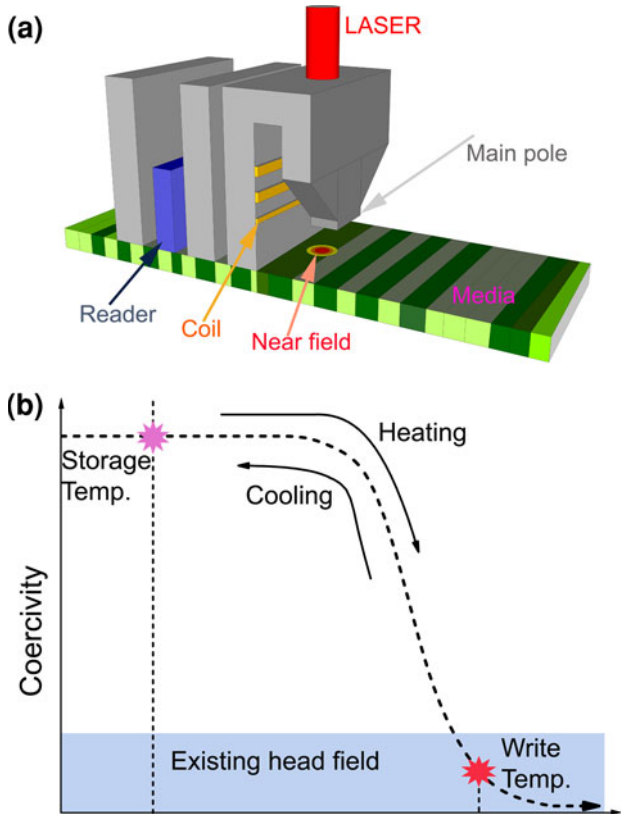

Fig. 3. (a) and (b) Schematic diagram of the HAMR and HAMR write process is shown.

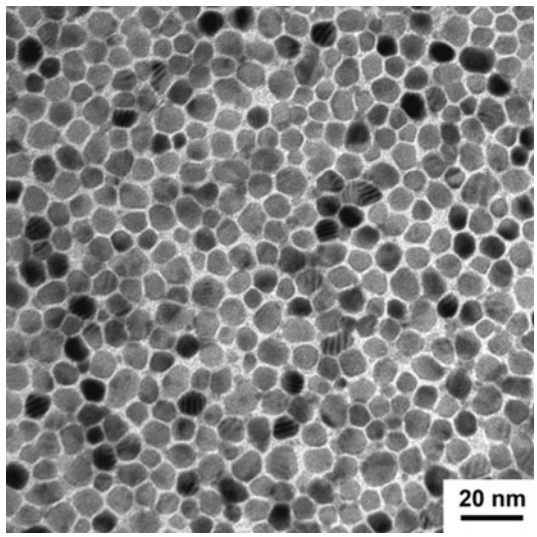

Fig. 4. Plane-view TEM image of the FePt-C granular thin film grown on an MgO underlayer on a thermally oxidized Si substrate. The first encouraging media structure with ~6 nm FePt particles uniformly dispersed with a narrow size distribution.[25]

has to be annealed above 640°C to make them transform to the $L1_0$ structure. For an industrially viable process, lowering the kinetic ordering temperature from the A1 to $L1_0$ structure is essential. Thus, many investigations to reduce the ordering temperatures by the addition of a third element to FePt have been carried out. For example, alloying with Cu and Ag were reported to reduce the ordering temperatures significantly in continuous polycrystalline films.[8–18] By alloying with Cu, the ordering temperature decreases to 400°C, whereas binary A1 FePt does not order below 600°C. The enhanced kinetics of ordering was attributed to the reduction of the melting temperature of the FePt phase by the Cu addition. Although the Cu can reduce the ordering temperature, the magnetocrystalline anisotropy energy deteriorates.[16] Also, the coarsening of the particle cannot be suppressed as long the ordering occurs by the volume diffusion. Note also that many early investigations were carried out on continuous polycrystalline films, where the ordering progress was accompanied by recrystallization.[17] Therefore the elements that are effective in reducing the ordering temperature do not necessarily works with the granular system where recrystallization is not expected.[17,18]

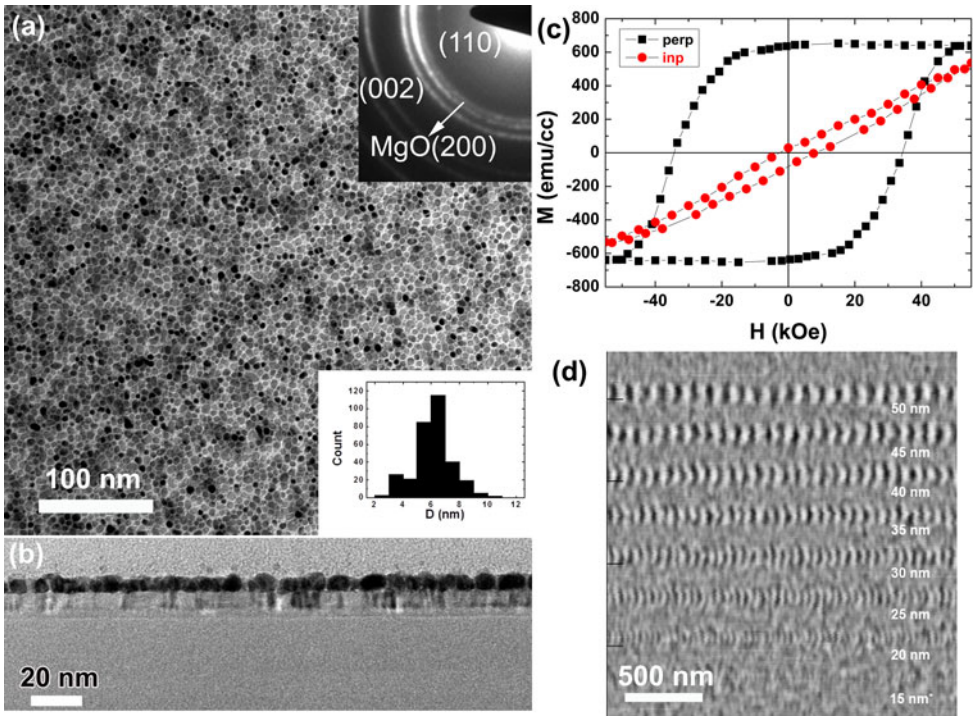

Fig. 5. (a) and (b) Plane-view and out-of-plane TEM image of the $(FePt)_{0.9}Ag_{0.1}$-40 vol.%C granular film and (c) magnetization curves. (d) The patterns of recording bits by the static HAMR head. The mean particle diameter of the FePt articles is 6.1 nm, and their size dispersion is 1.8 nm. Coercivity is 3.7 T, which is more than five times higher than that of the conventional magnetic recording media. In the recording pattern with the static HAMR head, 15-nm bits were observed with a bit width of 92 nm. Converted to a recording density, this is equivalent to 550 Gb psi.[28]

[001] Texture

To apply the $L1_0$-ordered FePt thin film to HAMR media, the magnetic easy axis must be aligned normal to the film plane. However, the FePt thin films deposited on amorphous substrates tend to develop a [111] texture because the (111) plane has the lowest surface energy. To realize a [001] texture, seed layers such as Cr, Ag, B_2O_3, and MgO have been explored.[19,20] Cr is one of the well-studied seed layers to induce FePt [001] texture. Although the (110) plane is the most close-packed plane in Cr, [001] texture developed at an optimized condition.[21] In addition, the lattice mismatch of 5.8% with the FePt (001) causes the expansion of the in-plane FePt (100) lattice. Because the c/a ratio of $L1_0$ FePt phase is 0.964, the slightly higher lattice mismatch between Cr (110) and FePt (100) assists the transformation from the A1 phase to the $L1_0$ phase. By adding Ru into Cr thin films, the lattice mismatch can be further controlled because the atomic radius of Ru is larger than that of Cr. Higher Ru concentration results in a larger lattice parameter of CrRu alloy following Vegard's law. Xu et al.[22] showed that 10 at.% Ru optimized the lattice mismatch for $L1_0$ formation. With in situ annealing, perpendicular FePt [001] texture with good $L1_0$ order was obtained at a relatively lower temperature of 350°C, whereas a temperature over 600°C was required to achieve good $L1_0$ ordering by postdeposition annealing. This means that a reduction of the ordering temperature by 200°C was achieved with the use of CrRu underlayer. Although a Cr-based underlayer reduces the ordering temperature, Cr diffusion into FePt deteriorates the magnetocrystalline anisotropy.

Among various seed layers, sputter-deposited MgO offers more advantages in seeding [001] oriented $L1_0$-FePt thin films.[23] MgO has a strong tendency to develop strong [001] texture during natural growth by sputtering, and FePt tend to grow epitaxially on MgO with the orientation relationship of $(001)_{MgO}//(001)_{FePt}$, $[001]_{MgO}//[011]_{FePt}$; thus, strong [001] texture develops on FePt magnetic layers on [001] textured MgO.

Granular Microstructure

Many investigations on the control of FePt nanogranular structure have been carried out using various kinds of segregants such as Al_2O_3, SiO_2, MgO, TiO_2, Ta_2O_5, and C. However, there had been no report on the uniform nanogranular microstructure that satisfies the specification for HAMR as shown in Fig. 2. When FePt is sputtered with oxides, the as-sputtered films have a uniform microstructure with very fine particle size of ~2 nm.[24] However, the FePt particles are disordered A1 phase, so they are superparamagnetic. When high-temperature annealing is applied for the $L1_0$ order, the coarsening and agglomeration of the particles

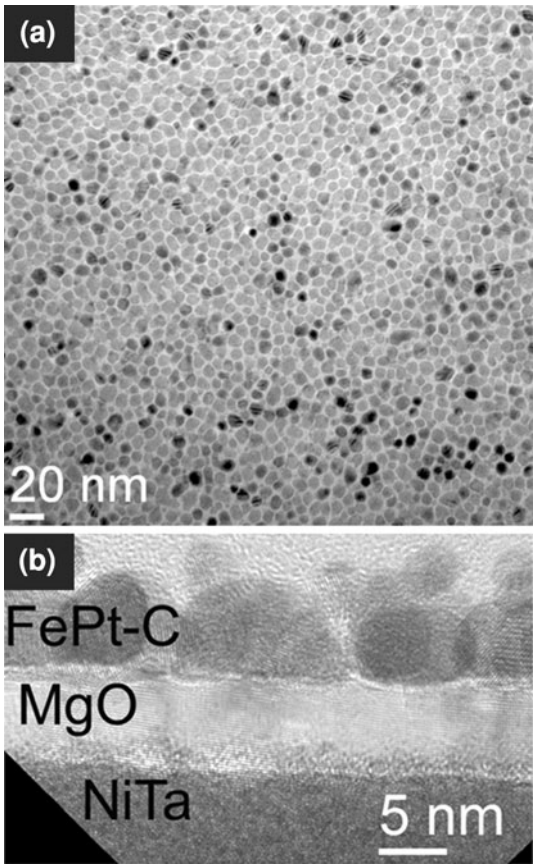

Fig. 6. (a) Plane-view and (b) out-of-plane TEM bright-field images of glass/*a*-NiTa (60 nm)/MgO (10 nm)/FePt-40 vol.%C (8 nm). The plane-view microstructure shows with ~5.8 nm FePt particles uniformly dispersed with a narrow size distribution, whereas the out-of-plane microstructure show a double-layered structure.[30]

occurs. All work on FePt-X films that were postdeposition heat treated showed such particle coarsening by the postdeposition heat treatment.

$(FePt)_{0.9}Ag_{0.1}$-C GRANULAR MEDIA FOR HAMR

Perumal et al.[25] reported a way to fabricate perpendicular magnetic thin films with FePt particles of a 5.5 nm mean diameter and a 2.3 nm size dispersion on thermally oxidized Si substrates using cosputtering of FePt-C on MgO seed layer. The key to the success was to sputter deposit FePt and C on a heated substrate so that the ordering to the $L1_0$ structure can progress during the film growth at a much lower temperature than that required for the postdeposition annealing (~640°C). During the growth of the films at an elevated temperature, atomic transport occurs by surface diffusion, thereby enhancing the kinetics for $L1_0$ ordering at a much lower temperature. Whereas $L1_0$ ordering progresses during the growth, carbon is rejected from FePt, forming a thin channel of amorphous carbon as shown in Fig. 4. However, the coercivity was only in the order of 0.8 T to 1.5 T due to the low

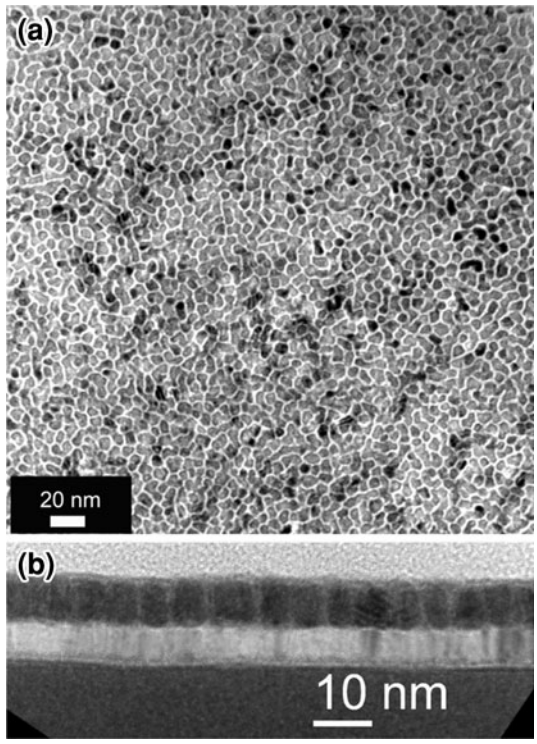

Fig. 7. (a) Plane-view and (b) out-of-plane TEM bright-field images of glass/*a*-NiTa (60 nm)/MgO (10 nm)/FePt-40 vol.%TiO_2 (8 nm). The out-of-plane microstructure shows good columnar structure with aspect ratio of ~2 with less surface roughness, whereas plane-view microstructure shows interconnected granular structure.[30]

degree of the $L1_0$ order in the FePt particles, and a higher coercivity had to be achieved for the HAMR media. Following the report by Platt et al.,[12] that the kinetic ordering temperature of FePt can be reduced by the addition of Ag, Zhang et al.[26] succeeded in processing a nanoparticle-dispersed perpendicular magnetic thin film with a mean particle diameter of 6.1 nm, size dispersion of 1.8 nm, and coercivity of 3.7 T by adding Ag to the FePt-C granular films. To align the [001] crystal orientation perpendicular to the film, a thin layer of MgO was grown on a Si substrate, followed by sputtering a (FePt)Ag-C magnetic layer. The $(FePt)_{0.9}Ag_{0.1}$-40 vol.%C film had the highest grade of particle dispersion and crystal alignment of $L1_0$-FePt particles. Figure 5a shows the in-plane transmission electron microscope (TEM) image, the selected area diffraction (SAED) pattern, and a particle size histogram. The in-plane TEM image shows the uniform microstructure with an average particle size of 6.2 nm and size distribution of 1.2 nm. The pitch distance (center to center) is about 9.6 nm. The SAED pattern shows the FePt particles have strong *c*-axis texture. Figure 5b shows the magnetization curves of out-of-plane and in-plane directions. The film has strong perpendicular anisotropy. The perpendicular $\mu_0 H_c$ is about 3.5 T, and an anisotropy field estimated by the cross point of the in-plane and out-of-plane curves is about 6.5 T. The estimated K_u

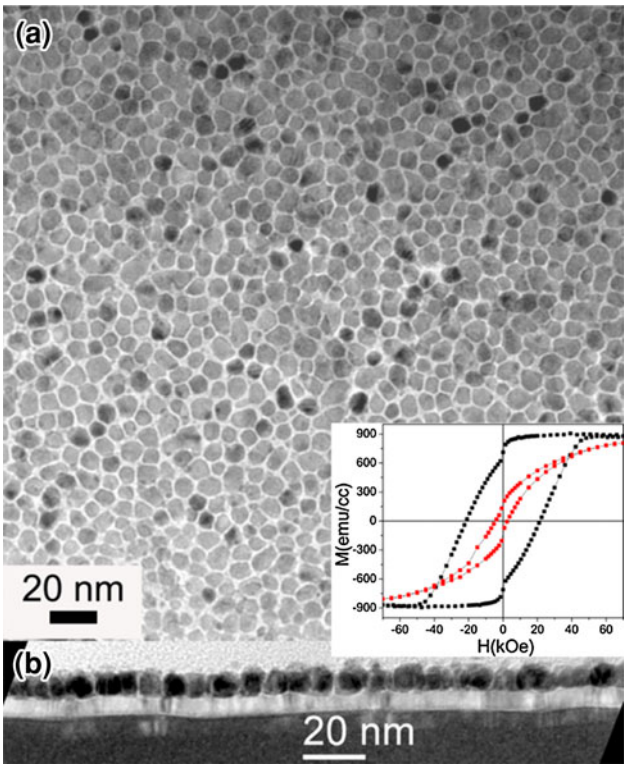

Fig. 8. (a) and (b) Plane-view and out-of-plane TEM bright-field images of glass/*a*-NiTa (60 nm)/MgO (10 nm)/FePt-50 vol.% (C, TiO_2) (8 nm) in inset perpendicular and in-plane magnetization curves are shown. The out-of-plane microstructure shows good columnar structure with aspect ratio of ~1.2 with less surface roughness compared with only carbon-containing films, and the plane-view microstructure shows well-separated granular structure.[30]

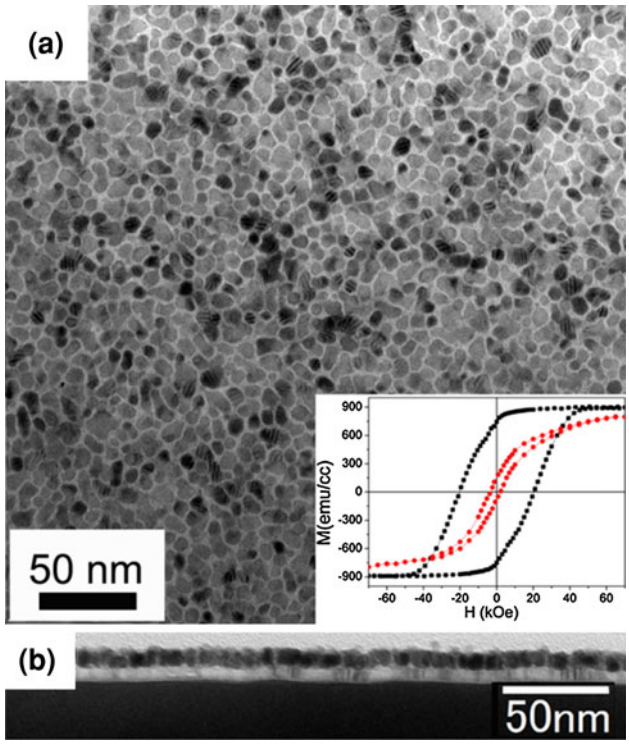

Fig. 9. (a) and (b) Plane-view and out-of-plane TEM bright-field images of glass/*a*-NiTa (60 nm)/MgO (10 nm)/FePt-40 vol.%C (4 nm)/FePt-40 vol.%TiO_2 (4 nm) perpendicular and in-plane magnetization curves were showed in inset. The out-of-plane microstructure shows columnar structure with an aspect ratio above 1 with less surface roughness compared with only carbon-containing films. The plane-view microstructure shows a well-separated granular structure. FePt-C as a template served to control the microstructure in lateral direction.[30]

of the FePt particles is 4.3×10^6 J/m^3, which is half of that in the bulk. The high K_u and $\mu_0 H_c$ result from the high degree of order in these films. The degree of $L1_0$ order was estimated to be 0.9 from the relative integrated intensity ratio of (002) and (004) in the x-ray diffraction (XRD) pattern. Because of the high-anisotropy FePt particles, the thermal stability ($K_u V/k_B T$) estimated by the time-dependent H_c measurement was about 200, indicating that this media was thermally stable for more than 10 years.[27] Subsequent HAMR static tester results demonstrated the areal density of 550 Gbit/in^2 on this medium as shown in Fig. 5c.[28] This recording density was the highest one achieved by HAMR at that time and was comparable to that of the conventional PMR method.

Because the (FePt)Ag-C nanogranular films can be deposited easily by sputtering on the MgO seed layer, where crystal orientations are naturally aligned to the [001] direction during the film growth, the (FePt)Ag-C films can be fabricated on substrates other than thermally oxidized Si, including glass substrates and amorphous metals. From this viewpoint, this technology has high potential to be extended to industrially viable production lines in the future and can be considered to be an important advancement toward the practical application of FePt-based HAMR media. Using a semi-industrial sputtering machine with a triode target, Hitachi Global Storage Technologies (San Jose, CA) reported similar microstructure with a slightly improved recording density grown on glass substrate with NiTa amorphous heat sink layer.[29]

Although the microstructure and magnetic properties attained in the (FePt)Ag-C was so close to that required for practical use, there have been two critical issues to be resolved: One is to obtain a small roughness on the surface and the other is to grow the FePt grains in a columnar shape with an aspect ratio $D/h > 1.5$ as shown in Fig. 2, whereas Fig. 6 shows the plane-view and cross-sectional image of FePt-C granular film grown on glass substrates. Although the plan-view image shows nice particle separation, the cross-sectional image shows the formation of a 2nd layer on top of the FePt particles that has grown epitaxially on the MgO seed layer. Because the 2nd layer does not have an orientation relationship with the underlayer separated by amorphous carbon, the perpendicular anisotropy is substantially degraded. This is because the C has a too strong driving force for phase separation. Although strong phase separation

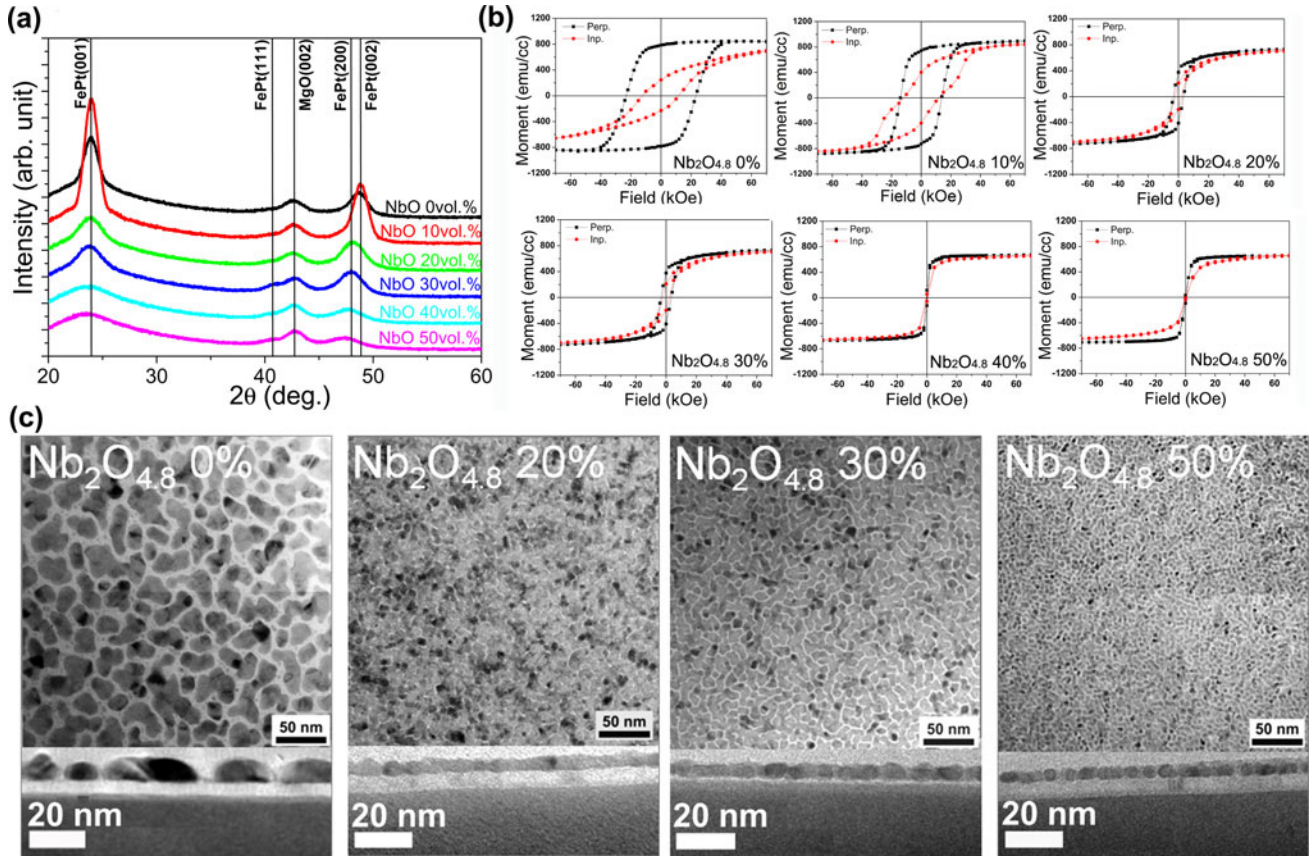

Fig. 10. (a) X-ray diffraction patterns of glass/*a*-NiTa (60 nm)/MgO (10 nm)/FePt-Nb_2O (*x* vol.%) films fabricated on glass substrates for $0 \le x \le 50$. (b) Perpendicular and in-plane magnetization curves of glass/*a*-NiTa (60 nm)/MgO (10 nm)/FePt-Nb_2O (*x* vol.%) films fabricated on glass substrates for $0 \le x \le 50$. (c) Plane-view and out-of-plane TEM bright-field images of glass/*a*-NiTa (60 nm)/MgO (10 nm)/FePt-Nb_2O (*x* vol.%). From XRD profiles and magnetization curves, it is evident that increase of Nb_2O volume fraction resulted in degrading $L1_0$ ordering, which means face-centered tetragonal to face-centered tetragonal structure. As Nb_2O volume fraction increases, the grain refinement is observed at 50 vol.% particles are well separated in both plane-view and out of plane, but the particles are in a spherical shape.[33]

makes the particle isolation better in the lateral direction, this in turn interrupts the columnar growth in the growth direction and causes another grain to nucleate on an underlying grain.

FePt-(C,MO_x) SYSTEM

Unlike the FePt-C system, FePt-SiO_2 and FePt-TiO_2 have been known to construct a good columnar structure, whereas the in-plane particle separation is very poor.[30,31] Figure 7 shows typical granular microstructure observed in the FePt-TiO_2 system. The FePt particles are interconnected in the planar direction, whereas a uniform columnar structure with a smooth surface is obtained in the cross-sectional view. However, the film showed soft magnetic properties because of the suppression of the $L1_0$ ordering due to the dissolution of Ti into FePt grains. This means that the driving force for the phase separation between FePt and SiO_2 or TiO_2 is too small to obtain well-isolated grains.

The in-plane interconnected microstructures in Fig. 7 suggest that the driving force for the phase separation of FePt with SiO_2 is too small. To optimize the driving force for the phase separation, Varaprasad et al.[30] mixed C and TiO_2. Figure 8 shows the in-plane and the cross-sectional TEM bright-field images and the magnetization curves of FePt-50 vol.%(C, TiO_2) film. Unlike Fig. 7 for FePt-TiO_2, a well-separated granular structure was obtained. The average particle size was 7.9 nm with the size distribution of 24%, which is slightly larger than the desired value. The cross-sectional TEM image shows the growth of single layer of FePt granular film. However, the magnetization curve of the out-of-plane direction shows a kink around the zero field even though H_c is high about 3 T. The kink is probably due to the presence of soft magnetic particles resulting from the dissolution of Ti into FePt. The microstructure is so close to the ideal one, and further optimization may lead to improved media structure.

As described above, FePt grains in the FePt-SiO_2 and FePt-TiO_2 systems show columnar structure, but the in-plane separation is not good enough.[30] To grow the columnar structure on well-isolated particles, Varaprasad et al.[30] attempted to grow

FePt-SiO_2 and FePt-TiO_2 granular films using well-isolated FePt-C thin granular films as templates. Figure 9a and b shows the in-plane and cross-section TEM bright-field images and the magnetization curves of the FePt-C/FePt-TiO_2 double-layered films. Although the H_c reduced to 15 kOe, the TEM images show well-separated columnar grains. This double-layer approach may lead to optimized columnar grain structure after further optimization of the growth conditions.

EXPLORATION OF A NEW FePt-X SYSTEM

As described above, carbon has an intrinsic weakness as a segregant, i.e., a too strong driving force for phase separation that interrupts the columnar growth and causes new grains to nucleate on the top surface. Although good surface roughness and columnar structure have been reported with a SiO_2 segregant,[32] planer particle separation is poor. These results suggest that the separating tendency of SiO_2 is too weak compared to that for carbon. Thus, the segregant whose driving force for phase separation is in-between C and SiO_2 could be an appropriate material for the columnar growth with good planar isolation. Based on this consideration, Shiroyama et al.[33] have explored several metal oxides MO_x as alternative segregants, which are expected to have a driving force for phase separation between those of carbon and SiO_2. They assumed that the solubility of MO_x decreases with the increase of the cohesive energy and explored the oxides whose cohesive energy is in between those for carbon and SiO_2, i.e., W, Nb, Zr, and Al.

As a typical example, the XRD patterns, magnetization curves, and TEM images of FePt-NbO_x granular films are shown in Fig. 10. All the films were deposited on glass disks with NiTa/MgO underlayer. With increasing the volume fraction of NbO_x, the degree of order and coercivity decreases. The microstructure changes from the network-like structure to the island structure with increasing NbO_x content. In the FePt-50 vol.% NbO_x film, several particles are interconnected in the planar direction having a smooth surface in the cross-sectional image. It suggests that the driving force for the phase separation of FePt with NbO_x is too small. In the granular film with other oxides, the tendencies of the magnetic properties and the microstructures with the increment of the oxide were similar. An energy-dispersive spectroscopy study of the FePt-50 vol.% NbO_x indicated that the Nb was dissolved in the FePt particles, which is considered to have caused the reduction of the thermodynamic $L1_0$ ordering temperature, thereby reducing the driving force for $L1_0$ ordering. The problem on using these oxides is the dissolution of the transition elements into FePt particles, which causes the low degree of ordering. To realize well-isolated columnar structure, the selection of elements that do not have low solubility with FePt seems to be necessary.

SUMMARY

Recent progress on the development of FePt granular films for HAMR media has been reviewed. Although (FePt)Ag-C granular films exhibited the microstructure marginally applicable as HAMR media, the system would not be the final answer for practical application due to the strong driving force of the phase separation between FePt and C, which causes a rough surface and hinders columnar growth. We need to find new segregants to realize well-isolated columnar growth. In addition to the control of the FePt recording layer, the development of the electrically conductive seed layers for the FePt texture control is required.

Seagate has recently announced a 1-Tbpsi HAMR recording probably by using FePt-based granular media, and the commercial implementation of HAMR appears to be right around the corner. However, further improvement of the microstructure to optimize the read and write properties as well as heat control is essential for achieving higher areal density beyond 2 Tbit/in^2 in HAMR.

ACKNOWLEDGEMENTS

We acknowledge the financial support for the work from Western Digital Inc. and IDEMA, ASTC.

REFERENCES

1. Y. Shiroishi, K. Fukuda, I. Tagawa, H. Iwasaki, S. Takenoiri, H. Tanaka, H. Mutoh, and N. Yoshikawa, *IEEE Trans. Magn.* 45, 3816 (2009).
2. T. Klemmer, D. Hoydick, H. Okumura, B. Zhang, and W.A. Soffa, *Scripta Metall. Mater.* 33, 1793 (1995).
3. D. Weller and A. Moser, *IEEE Trans. Magn.* 35, 4423 (1999).
4. R.E. Rottmayer, S. Batra, D. Buechel, W.A. Challener, J. Hohlfeld, Y. Kubota, B. Lu, C. Michalcea, T. Rausch, M.A. Seigler, and X.M. Yang, *IEEE Trans. Magn.* 42, 2417 (2006).
5. D. Guarisco and H. Nguy, *J. Appl. Phys.* 93, 6745 (2003).
6. B.C. Stipe, T.C. Strand, C.C. Poon, H. Balamane, T.D. Boone, J.A. Katine, J.L. Li, V. Rawat, H. Nemoto, A. Hirotsune, O. Hellwig, R. Ruiz, E. Dobisz, D.S. Kercher, N. Robertson, T.R. Albrecht, and B.D. Terris, *Nature Photon.* 4, 484 (2010).
7. M.H. Kryder, E.C. Gage, T.W. McDaniel, W.A. Challener, R.E. Rottmayer, G. Ju, Y.T. Hsia, and M.F. Erden, *Proc. IEEE* 96, 1810 (2008).
8. T. Maeda, A. Kikitsu, T. Kai, T. Nagase, and J. Akiyama, *Appl. Phys. Lett.* 80, 2147 (2002).
9. Y.K. Takahashi, M. Ohnuma, and K. Hono, *J. Magn. Magn. Mater.* 246, 259 (2002).
10. O. Kitakami, Y. Shimada, K. Oikawa, H. Daimon, and K. Fukamichi, *Appl. Phys. Lett.* 78, 1104 (2001).
11. C. Chen, O. Kitakami, S. Okamoto, and Y. Shimada, *Appl. Phys. Lett.* 76, 3218 (2000).
12. C.L. Platt, K.W. Wierman, E.B. Svedberg, R. Veerdonk, J.K. Howard, A.G. Roy, and D.E. Laughlin, *J. Appl. Phys.* 92, 6104 (2002).
13. S.R. Lee, S. Yang, Y.K. Kim, and J.G. Na, *J. Appl. Phys.* 91, 6857 (2002).
14. K. Nishiyama, K. Takahashi, H. Uchida, and M. Inoue, *J. Magn. Magn. Mater.* 272, 2189 (2004).
15. T. Shima, T. Moriguchi, S. Mitani, and K. Takanashi, *Appl. Phys. Lett.* 80, 288 (2002).
16. M. Maret, C. Brombacher, P. Matthes, D. Makarav, N. Boudet, and M. Albercht, *Phys. Rev. B* 86, 024204 (2012).
17. Y.K. Takahashi, M. Ohnuma, and K. Hono, *Jpn. J. Appl. Phys.* 40, L1367 (2001).

18. Y.K. Takahashi and K. Hono, *Scripta Mater.* 53, 403 (2005).
19. Y.F. Ding, J.S. Chen, E. Liu, C.J. Sun, and G.M. Chow, *J. Appl. Phys.* 97, 10 (2005).
20. J.-G. Zhu, X. Zhu, and Y. Tang, *IEEE Trans. Magn.* 44, 25 (2008).
21. T. Maeda, *IEEE Trans. Magn.* 41, 3331 (2005).
22. Y. Xu, J.S. Chen, and J.P. Wang, *Appl. Phys. Lett.* 80, 3325 (2002).
23. S. Jeong, M.E. McHenry, and D.E. Laughlin, *IEEE Trans. Magn.* 37, 1309 (2001).
24. D.H. Ping, M. Ohnuma, K. Hono, M. Watanabe, T. Iwasa, and T. Masumoto, *J. Appl. Phys.* 90, 4708 (2001).
25. A. Perumal, Y.K. Takahashi, and K. Hono, *Appl. Phys. Exp.* 1, 101301 (2008).
26. L. Zhang, Y.K. Takahashi, A. Perumal, and K. Hono, *J. Magn. Magn. Mater.* 322, 2658 (2008).
27. L. Zhang, Y.K. Takahashi, K. Hono, B.C. Stipe, J.Y. Juang, and M. Grobis, *J. Appl. Phys.* 109, 07B703 (2011).
28. L. Zhang, Y.K. Takahashi, K. Hono, B.C. Stipe, J.Y. Juang, and M. Grobis, *IEEE Trans. Magn.* 47, 4062 (2011).
29. O. Mosendz, S. Pisana, J.W. Reiner, B. Stipe, and D. Weller, *J. Appl. Phys.* 111, 07B729 (2011).
30. B.S.D.Ch.S. Varaprasad, M. Chen, Y.K. Takahashi, and K. Hono, *IEEE Trans. Magn.* 49, 718 (2013).
31. A. Perumal, Y.K. Takahashi, T.O. Seki, and K. Hono, *Appl. Phys. Lett.* 92, 132508 (2008).
32. E. Yang and D.E. Laughlin, *J. Appl. Phys.* 104, 023904-1 (2008).
33. Y. Shiroyama, Y.K. Takahashi, and K. Hono, *IEEE Trans. Magn*. Accepted for publication.